System Architecture of a Reusable N2O/Paraffin-ABS Hybrid Rocket Lander

Szu Heng Chen*, Jack R. Rumpf†, Michael Swoyer*, Anyi X. Lin‡, Suhaila Rashid§, Udita Mahajan§, Herris Fentress*, Hanming Sun¶, Alexis Alfonseca†
Georgia Institute of Technology, Atlanta, Georgia, 30332

Reusable rocket technology, since its adoption, has drastically altered the trajectory of the aerospace industry. Rockets that can be recovered then reflown not only lower the cost of launching payloads into space but also enable a significantly higher launch cadence that is incompatible with traditional expendable launch vehicles. Despite this remarkable progress at the industrial scale, collegiate rocketry efforts have largely evolved along a separate trajectory. More often than not, success is evaluated using apogee-centric criteria, which have shaped student launch vehicle architectures toward expendable designs optimized for a single flight with little to no consideration for reusability. With this in mind, Propulsive Landers at the Georgia Institute of Technology (GTPL) was established as the first student organization at Georgia Tech to pursue vertical takeoff and vertical landing (VTVL) rocket flight. The program's short-term focus is the development of a 1000N-class VTVL lander with a flight envelope consisting of a 10s tethered hover, an untethered 10m powered descent, and an untethered 50m vertical hop. The purpose of these objectives is to reframe student rocketry around the constraints of reusability and to offer early exposure to the engineering challenges present in modern reusable launch vehicle development.This paper presents the system architecture adopted by GTPL in the development of this lander. Mission definition, system and subsystem requirements, and the baseline vehicle configuration are described along with primary design drivers and tradeoffs.

I. Introduction

In the past two decades, student rocketry has quickly matured into an organized and technically demanding ecosystem that has pushed teams to achieve what was once thought impossible at the student scale. The Spaceport America Cup, for example, is the world's largest Intercollegiate Rocket Engineering Competition. Teams fly to 10,000ft or 30,000 ft across 6 categories, with criteria covering design and construction, technical reports, and deviation from apogee [1]. In its 2024 event alone, there were a total of 6153 participating students across 152 teams which represented over 20 countries combined [2]. Around the world, there are also other rising initiatives like the Europe's own European Rocketry Challenge (EuRoC) hosted by the Portuguese Space Agency and Taiwan Space Agency (TASA)'s Rocket Taiwan cup [3]. Despite this rapid growth, the dominant metric of "success" in most collegiate programs are apogee-centric. Many teams compete to be the first to across the Karman Line in its propulsion categories, while others compete for a targeted altitude. While the underlying approach is highly effective at developing fundamentals involving structural design and recovery, propulsion systems development, and avionics, it still overlooks many of the relevant skills needed to build the reusable, autonomous vehicles we see today.

Today's missions are no longer Shown in centered around purely ascent-and-recovery. With Falcon 9's routine booster recovery and now the Super Heavy Booster by the launch tower's mechanical arms, SpaceX has shown reusability is a practical reality [4]. Blue Origin has also pursued an analogous approach in the suborbital and now orbital regime with New Glenn's successful first stage landing as of November, 2025 [5]. The European Space Agency (ESA) is also developing their Themis (TH1) reusable stage demonstrator explicitly intended to prove Europe's vertical takeoff and vertical landing (VTVL) abilities [6]. Likewise in China, LandSpace has progressed toward the same end state with its Zhuque-3 program [7]. Together, these efforts reflect a broader paradigm shift where performance is increasingly evaluated not only by ascent performance but also other metrics, including autonomous recovery and turnaround, that are all driven by the concept of reusability.

*Undergraduate Student, Guggenheim School of Aerospace Engineering, Atlanta, GA, 30332, AIAA University Student.
†Undergraduate Student, Woodruff School of Mechanical Engineering, Atlanta, GA, 30332, AIAA University Student.
‡Undergraduate Student, College of Computing, Atlanta, GA, 30332, AIAA University Student.
§Undergraduate Student, School of Electrical and Computer Engineering, Atlanta, GA, 30332, AIAA University Student.
¶Undergraduate Student, School of Industrial Design, Atlanta, GA, 30332, AIAA University Student.

Motivated by this gap, Propulsive Landers at the Georgia Institute of Technology was established over a year ago with the vision to pursue a VTVL demonstrator that, in the future, can execute the same complex algorithms used to land on other planets. Students on the team are challenged by system integration where one change can no longer be made without considering the effects on the system. Now, they must consider (1) how to throttle their engine and through what mechanism (2) how to estimate state reliability under external influences (3) how to design guidance and control laws that remain stable through the entire phase of flight (4) how must the system be verified before a full commitment to flight.

II. Mission Definition and System Architecture

A. Mission Definition and Requirements

The near-term mission of the vehicle is to demonstrate controlled vertical takeoff, hover, and landing in a staged manner. The first milestone consists of a tethered hover demonstration. This phase is intentionally constrained to provide a controlled environment for validating throttle mechanism and state estimation without committing to a free flight. Following successful tethered hover, the program proceeds to a 10 m drop followed by a 50 m vertical hop demonstration. Mission-level requirements were derived directly from the staged flight envelope, shown in Table 1, and reflect the primary objective of demonstrating controlled and repeatable VTVL operation. These demonstrations impose system-level constraints on propulsion throttle authority, closed-loop stability, state estimation performance, and safety architecture, which collectively define the vehicle's minimum functional capabilities as reflected in Table 2.

Table 1 Mission Profile Operating Envelopes

Tethered Hover	
Target altitude	0–2 m
Profile duration	10 s
Landing zone radius	0.5 m
Touchdown velocity	0.5 m/s
Profile type	Tethered

10 m Hop	
Target altitude	10 m
Profile duration	30
Landing zone radius	≤ 1 m
Touchdown velocity	≤ 0.5 m/s
Profile type	Free flight

50 m Hop	
Target altitude	50 m
Profile duration	40
Landing zone radius	≤ 1 m
Touchdown velocity	≤ 0.5 m/s
Profile type	Free flight

Table 2 Mission-Level Requirements

Req ID	Mission-level requirement	Verification means	Applies to
M-01	The vehicle shall support the near-term missions consisting of tethered hover, an untethered 10 m vertical hop, and an untethered 50 m hop with controlled landing.	Demonstration (flight)	All
M-02	The vehicle shall maintain stable closed-loop attitude control throughout ascent, hover, and descent.	Demonstration (flight), Analysis	All
M-03	The vehicle shall land within a predefined landing zone for each untethered hop demonstration.	Demonstration (flight)	10 m, 50 m
M-04	The propulsion system shall provide throttle authority within 50–100% commanded throttle.	Test, Analysis	All
M-05	The vehicle shall provide real-time state estimation (position, velocity, attitude, and angular rates) at a rate compatible with the control loop accounting for latency.	Analysis, Test, Demonstration (flight)	All
M-06	The vehicle shall constrain touchdown conditions within program-defined allowable limits listed in table.	Demonstration (flight), Analysis	10 m, 50 m
M-07	The system shall incorporate a flight-terminating capability which can command an emergency shutdown and place the vehicle in a safe state under off-nominal conditions if necessary.	Test, Demonstration (flight)	All
M-08	The vehicle shall record telemetry sufficient to reconstruct flight and allow post-processing for further flight analysis and model validation.	Inspection, Test	All

B. Baseline System Architecture

The baseline vehicle, shown in Fig. 1, consists of a 1000N hybrid rocket engine, a two-axis thrust vector control system for pitch and yaw, an aluminum 6061 N2O main tank, four nitrogen carbon fiber tanks, and a dedicated cold gas reaction control system for roll (not shown in figure), and an onboard avionics bay responsible for state estimation and control. The thrust 1000N thrust class was deliberately selected as a small-scale demonstrator that can be tested iteratively at low cost while still producing a sufficient thrust-to-weight ratio for hover and hop profiles.A summary of the vehicle configuration can be found in Table 3. The sections that follow examine each subsystem in detail, including propulsion, avionics, and guidance, navigation, and control. For each subsystem, primary design drivers, key trade considerations, and the rationale behind selected configurations are presented. Emphasis is placed on how subsystem-level decisions were shaped by mission constraints and how their integration enables closed-loop VTVL operation.

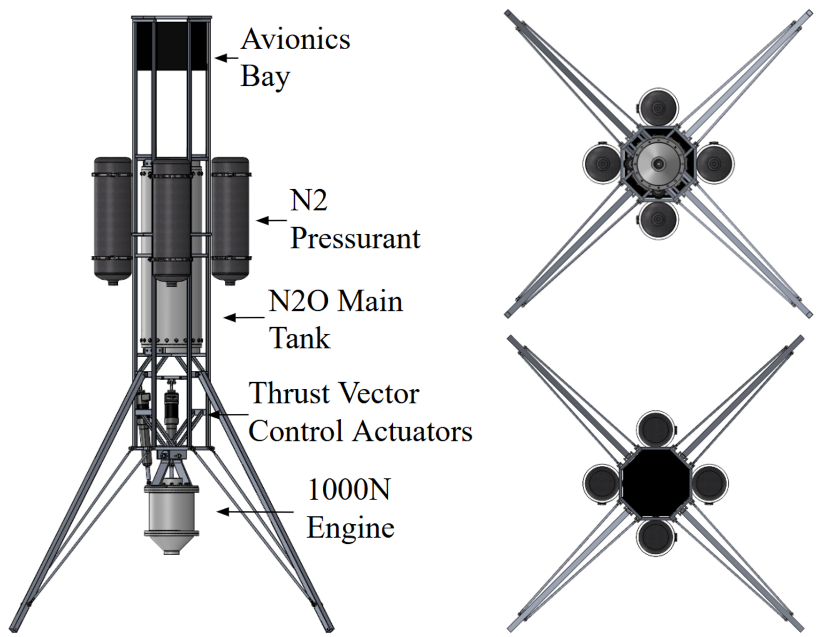

Fig. 1 Design of 1000N Vehicle

Table 3 Baseline Vehicle Configuration Summary

Parameter	Value
Vehicle class	1000 N VTVL hybrid lander
Propulsion	Regulated N_2O/Paraffin–ABS hybrid
Throttling method	Chamber-pressure feedback
Throttle capability	2.5:1 (40–100% of rated thrust)
Attitude control (pitch/yaw)	Two-axis TVC)
Attitude control (roll)	N_2 cold-gas RCS
Avionics architecture	Fully onboard state estimation and control

III. Propulsion System

A. Propulsion Subsystem

The propulsion subsystem provides the thrust needed for ascent and descent for flight. This section presents the propulsion requirements, as shown in Table 4, and highlights the key architecture trades, and the eventual feed system configurations that were selected to satisfy the aforementioned VTVL mission profiles. In this process, emphasis was placed on throttling feasibility, feed system stability, and repeatable test operations.

Table 4 Propulsion Subsystem Requirements

Req ID	Propulsion-level requirement	Verification means	Applies to
P-01	The propulsion system shall produce 1000 N-class maximum steady-state thrust at nominal operating conditions.	Test (static fire), Analysis	All
P-02	The propulsion system shall provide commanded throttle authority over the range 40–100% of rated thrust.	Test, Demonstration (flight)	All
P-03	The propulsion system shall regulate chamber pressure to track commanded setpoints.	Test, Analysis	All
P-04	The Main Throttle Valve (MTV) shall provide repeatable flow control over the full throttle range without destabilizing onboard closed-loop control.	Test (bench and hot-fire), Inspection	All
P-05	The propulsion system shall achieve throttle transitions with a dynamic response compatible with the vehicle control bandwidth by GNC analysis.	Test (step response), Analysis	All
P-06	The propulsion system shall provide a commanded engine shutdown capability that transitions the system to a safe state under nominal conditions.	Test, Demonstration (flight)	All
P-07	The oxidizer feed system shall maintain continuous and stable oxidizer delivery across the throttle range without unstable starvation or flow oscillations.	Test, Analysis	All
P-08	The propulsion system shall maintain chamber pressure, feed pressure, and critical temperatures within program-defined allowable limits during operation.	Test, Analysis	All
P-09	The engine shall demonstrate stable combustion behavior across the throttle range without sustained instability exceeding allowable amplitude thresholds ±5% of desired throttle.	Test (instrumented hot-fire), Analysis	All
P-10	The propulsion system shall demonstrate a minimum burn duration sufficient to support the tethered hover and vertical hop flight envelopes.	Test, Demonstration (flight)	All

B. Design Drivers and Architecture Overview

The propulsion architecture for the VTVL lander was driven by a combination of controllability, reusability, and system integration constraints. On one hand, the vehicle must regulate thrust continuously, and reliably throughout ascent, hover, and descent. On the other, it also must be functional and cheaply repeatable across tests. These combined objectives shaped the selection of feed architecture, propellant combination, operating pressure, and throttling mechanism which the section explores with reason.

1. Propulsion Architecture Selection

The selection of propulsion category was driven by considerations of cost, logistics, operational safety, in that order. For a VTVL lander, thrust must be actively adjusted throughout ascent, hover, and descent. Solid rocket motors, while mechanically simple, do not provide throttle authority and were therefore incompatible with the mission profile. Liquid bipropellant engines offer high performance and precise changes in thrust at the price of cost especially when considering the combined costs of infrastructure and [8]. With the reasons mentioned, hybrids were ultimately chosen as it offers the throttle capability without incurring the cost of full infrastructure. The absences of cryogenic fluids also removes the need for insulated storage, chill down procedures and cryogenic-rated ground support equipments. In addition, the use of an inert solid fuel eliminates the risks of unintended liquid-liquid mixing during startup.

2. *Oxidizer Selection and Feed Architecture*

Given any rocket system, mass is a critical driver of performance. For that purpose nitrous oxide was selected as the oxidizer due to its high density [9]. Beyond density considerations, nitrous oxide was chosen due to its self-pressurizing behavior in the saturated two-phase regime. This, theoretically, eliminates the need for an external pressurization system that reduces the system complexity and mass [10]. However, while self-pressurization offers architectural advantages, it also introduces feed system complexities that directly impact throttling feasibility. In a purely self-pressurized system, tank pressure evolves dynamically as oxidizer mass is depleted. As the tank depletes, effective pressure differential across the injector changes which alters the oxidizer mass flux independently of the commanded valve position. Therefore, despite the architectural advantages offer by a blowdown configuration, near-term feasibility and controllability considerations led to a regulated feed approach. In this system, nitrous is externally pressurized to a pressure above saturation pressure. Under subcooled conditions the oxidizer exists as a single-phase liquid rather than a vapor-liquid mixture. This eliminates the dependence on ambient temperature as a factor in saturated equilibrium and decouples feed system behavior from thermodynamic transitions during depletion. As a result, upstream pressure remains substantially stable throughout the burn and change in pressure becomes primarily a function of MTV position as opposed to evolving tank dynamics [11].

3. *Fuel Selection and Grain Configuration*

On the fuel side, we have chosen to use paraffin due to its inherent high regression rate compared to conventional polymeric fuels such as HTPB, PMMA, and HDPE [12]. The increased regression rate allows higher fuel mass flow rates and thus a reduced L/D ratio relative to its counterparts [13]. To improve manufacturability and repeatability, the paraffin is casted within an ABS gyroid. This has been previously referenced as "Armored Grain," and explored by Bisin et al. [14]. The ABS gyroid eliminates the need for external metal molds and releases coatings which would otherwise be necessary if it were paraffin wax alone [15]. The entirety of the process is also much simpler compared to other fuels such as HTPB that require multi-step procedures involving precision molds, cure cycles, and de-molding processes all of which introduce additional variability and labor overhead [16]. ABS was chosen due to its glass transition temperature of 105 °C that sits right above the casting temperature within the range of 80-100 °C [17].

C. Engine and Feed System Design

The engine is a 1000 N nitrous oxide/paraffin–ABS hybrid rocket engine at the maximum operating pressure of 55 bar with an upstream tank pressure of 65 bar. A high chamber pressure was chosen to improve the combustion efficiency of paraffin wax given rise by its droplet entrainment mechanism [12]. The 65 bar tank pressure maintains nitrous oxide in a single-phase, subcooled liquid state throughout the feed system to prevent flashing within feed lines. A showerhead injector with a 8 bar pressure drop (15% of chamber pressure) was used to maintain a relatively more uniform burn (compared to swirl injectors) and achieve the required injector differential pressure across the throttle range to decouple feed system dynamics [18]. A short pre-combustion chamber is included upstream of the fuel grain to increase combustion efficiency and allow the measurement of chamber pressure for throttling [19]. The engine is sized for 40 seconds of full thrust. The 40 seconds originated from lossless path analysis, with margin for transients and corrections, to profiles up till the 50 m powered descent. Though, the current casing is limited to only 10 seconds of operation. The primary limitation arises from thermal conduction from the graphite nozzle insert into the aluminum chamber. Given that the chamber is not actively cooled, thermal soak during extended burns would exceed the allowable structural temperature limits. As such, the engine is bounded to short-duration tests while propulsion changes are being made. To enable the full 40-second duration, modular ablative nozzle inserts are under development to increase thermal margin and reduce conductive heat transfer into the structural casing. A summarizing table of engine properties is shown in Table 5.

D. Throttle Mechanism

Throttle control in a nitrous, even in an externally pressurized, system presents unique challenges due to the coupled dynamics between oxidizer mass flow, evolving port geometry, and thereby change in O/F ratio and thrust throughout course of flight. Unlike liquid bipropellant engines, only oxidizer is directly actuated in a hybrid system. Fuel mass flow on the other hand is only an indirect response that is a combination of factors including instantaneous port surface area and regression rate. From a control standpoint, there are two primary strategies which exist for regulating thrust in such a system. The first is a model-based approach in which oxidizer mass flow is commanded through the throttle valve

Table 5 Engine Parameters

Parameter	Value
Maximum steady-state thrust, F_{max}	1000 N
Throttle ratio	2.5:1
Maximum Chamber pressure, p_c	55 MPa
Regulated tank pressure, p_{tank}	6–6.5 MPa
Injector pressure drop, Δp_{inj}	0.8 Mpa
Average mixture ratio, O/F	7.1
Specific Impulse, I_{sp} (sea level)	215 s
Specific Impulse Efficiency, ηIsp (sea level)	0.8
Design burn duration	40 s

while fuel mass flow is estimated using regression-rate correlations. In this approach, the required thrust is calculated using oxidizer mass flow rate, predicted fuel regression, O/F ratio, and nozzle expansion relations (assuming a change in nozzle diameter due to erosion) [20]. By this relation, the throttle valve angle is then adjusted to achieve the desired thrust. The advantage of this approach is that it attempts to directly regulate the variable of interest through an explicit physical representation of the combustion process. Assuming that the regression correlations are well characterized, this could provide accurate thrust predicted especially at the beginning of burn where geometry and thermodynamic states are known with high confidence. Another advantage the architecture brings is that it offers the physical transparency and theoretical states of the sysstem as variables are tracked throughout the entire course of flight. In principle, such a model-based controller could anticipate changes in thrust due to geometry evolution rather than reacting to them.

However, this predictive capability comes at the cost of increased computational complexity and model dependence. Because regression rate correlations are empirical and strongly dependent on oxidizer mass flux, port geometry, and flow conditions, small deviations between modeled and actual behavior can propagate throughout the burn [21]. Over extended burn durations, this uncertainty accumulates and require continual re-characterization across throttle ranges. The controller therefore becomes tightly coupled to the fidelity of the regression model which is not necessarily scalable across systems. While rigorous, such an approach places significant burden on modeling accuracy and tracking of time-varying states. For a reusable student-scale lander operating across iterative test cycles, this dependence on evolving regression characterization introduces both integration risk and extended development timelines.

In contrast, the present architecture adopts a pressure-regulated control philosophy that reduces reliance on real-time regression modeling and instead anchors thrust control to a directly measurable combustion state. The throttle approach adopted for our vehicle follows the closed-loop throttling framework previously demonstrated by Whitmore et al. and Peterson et al. [22]. Here, thrust is regulated through the control of the oxidizer mass flow rate with chamber pressure as the feedback variable. This control is achieved by a component named the Main Throttle Valve (MTV) upstream of the injector, and consists of a 60 degree v-port ball valve actuated by a high torque motor which adjusts the angle of the valve to the angle commanded. A v-port ball valve was selected with hopes of reducing the strong non-linearity typically associated with standard ball valve coefficients especially near small opening angles. A defining characteristic of this architecture is that it intentionally collapses a full chamber dynamics model into chamber pressure within the control loop. Any change in behavior appears as a deviation in chamber pressure and an external PID loop corrects it through feedback with appropriate tuning [22]. This makes the throttle architecture scalable across flight profiles. Our range of throttle was selected conservatively based on the results of Whitmore et al. and Peterson et al. Both throttling demonstrations achieved a stable throttle regime down to a 66:1 turndown ratio Further details related to the design of the controller can be found in the section below.

IV. Avionics, and Guidance, Navigation, and Control (GNC)

A. Avionics Subsystem

The avionics subsystem encompasses all of the necessary electronics for sensor data acquisition, control, and actuation. Our avionics system consists of an onboard computer, the Jetson Orin Nano, and several sensors in an isolated avionics bay: a VectorNav dual Global Navigation Satellite System/Inertial Navigation System (GNSS/INS), a 9-axis Inertial Measurement Unit (IMU), a Ultra-Wideband (UWB) sensor, and pressure transducers. Our main navigational sensor is the VN-300 dual GNSS/INS system from VectorNav, which was chosen due to its minimal sensor drift, accuracy, and robustness to magnetic interference. The DWM1000 UWB module is used to obtain altitude with centimeter-level accuracy during descent. The InvenSense ICM-20948 9-axis IMU serves as a redundant sensor in the unlikely circumstance of VN-300 or DWM1000 failure. The navigational sensors transmit data using Serial Peripheral Interface (SPI) through a communications board. The pressure transducers output an analog signal, which is fed into a custom data acquisition board responsible for filtering and analog-to-digital conversion. The majority of our sensor data is transmitted to our Ground Control Station for post-processing with the exception of our engine pressure, which is transmitted to our onboard computer during flight. Our avionics system is also responsible for the actuation of our Main Throttle Valve (MTV) and additional ball valves in our feed system. To maintain a high-level overview of our sensor architecture, we have chosen to omit detailed power budget information in this overview. The ultimate goal of our avionics subsystem is to supply GNC real-time data to make informed decisions on the flight state and trajectory.

B. GNC Subsystem

The GNC subsystem is responsible for the logic that controls the vehicle. It is divided into 3 main parts: state estimation, control, and navigation. To obtain an accurate state estimation, we must transform raw, noisy sensor data into a clean estimate at the ground truth. We must keep track our position, velocity, attitude, and angular velocity in order to provide our control algorithms with a strong basis to operate from. Our control algorithms are responsible for commanding our thrust vector control (TVC) and reaction control system (RCS) to maintain the vehicle's stability and move the vehicle to our desired position. Our control algorithms don't optimize over the entire flight profile due to their focus on detailed immediate control, so we need the navigation algorithms to provide optimal trajectories to target in order to minimize our fuel usage. All these algorithms are unified under our control loop, which is also responsible for communication to our ground station. To achieve these goals, we define requirements as shown in Table 6.

Table 6 AGNC Subsystem Requirements

Req ID	GNC-level requirement	Verification means	Applies to
G-01	The control algorithms shall maintain the vehicle's position within a 1 meter radius of the intended position.	Test (simulation, tethered hover), Demonstration (flight)	All
G-02	The control algorithms shall land with a vertical velocity of no more than 0.5 meters per second.	Test (simulation, tethered hover), Demonstration (flight)	All
G-03	The sensor fusion algorithms shall estimate the vehicle's attitude at a frequency of at minimum 300 Hz.	Test (simulation, tethered hover), Demonstration (flight)	All
G-04	The sensor fusion algorithms shall estimate the vehicle's attitude to an accuracy of within 0.5 degrees.	Test (simulation, tethered hover), Demonstration (flight)	All
G-05	The sensor fusion algorithms shall estimate the vehicle's position at a frequency of at minimum 10 Hz.	Test (simulation, tethered hover), Demonstration (flight)	All
G-06	The sensor fusion algorithms shall estimate the vehicle's position at an accuracy of within 0.1 meters.	Test (simulation, tethered hover), Demonstration (flight)	All
G-07	The control algorithms shall maintain the vehicle's roll angle within 5 degrees of the starting angle with the Reaction Control System.	Test (simulation, tethered hover), Demonstration (flight)	All
G-08	The thrust vector control module shall actuate at a minimum angular speed of 60 degrees per second.	Test (simulation, tethered hover), Demonstration (flight)	All
G-09	The thrust vector control module shall actuate to a minimum of 15 degrees from the vertical.	Test (simulation, tethered hover), Demonstration (flight)	All

Req ID	GNC-level requirement	Verification means	Applies to
G-10	The throttle control algorithm shall actuate the Main Throttle Valve to within 5% of the demanded thrust.	Test (simulation, tethered hover), Demonstration (flight)	All
G-11	The navigation algorithms shall produce an optimal trajectory at a frequency of at minimum 0.2 Hz.	Test (simulation, tethered hover), Demonstration (flight)	10 m, 50 m
G-12	The vehicle shall maintain constant communication with the ground station to a range of at minimum 1 kilometer.	Test (simulation, tethered hover), Demonstration (flight)	All
G-13	The control loop shall enable all the aforementioned algorithms to run at their specified speeds concurrently.	Test (simulation, tethered hover), Demonstration (flight)	All
G-14	The vehicle shall terminate flight whenever conditions become unsafe or commanded to by the ground station.	Test (simulation, tethered hover), Demonstration (flight)	All

C. State Estimation Considerations

For any control system, accurate state estimation is crucial for maintaining optimal control. Therefore, our sensor fusion algorithms are vital to the proper operation of the vehicle. However, the vehicle itself is a challenging environment for accurate sensor measurements, with significant vibrational noise from the engine and reaction control system (RCS), as well as significant magnetic interference from actuators and wiring. Inertial measurement units (IMUs) are commonly used to estimate attitude through a combination of gyroscope, accelerometer, and magnetometer readings, all of which can be affected by the aforementioned noise. Therefore, our sensor fusion algorithms must be robust, accurate, and quick. Angular dynamics change far more rapidly than translational dynamics. Therefore, it is most important that our vehicle maintains a precise attitude estimate. To maintain stable hovering and prevent undesirable behavior, such as rapid unscheduled disassembly, during the landing phase, the attitude estimate must be accurate to within half of a degree of the actual attitude. In order to maintain such an accurate attitude, our attitude estimation algorithms must update rapidly at a rate of at least 300 Hz.

We must also have accurate position estimates to maintain a hover without drifting out of our position bounds. Positional sensors update far less frequently than IMUs, typically between 10 and 50 Hz, requiring filtering algorithms to provide positional estimates fast enough for use in our control algorithms. It is possible to estimate position from a double integration of the accelerometer in the IMU, but the accelerometer is noisy and therefore results in rapid drift in the position estimate. Commonly used sensors like Global Positioning System (GPS) or other Global Navigation Satellite Systems (GNSSs) provide meter-level position estimates but without being bound to a ground station. To improve this estimate, methods such as real-time kinematic (RTK) can be employed which improve this accuracy to centimeter-level accuracy but with a dependency on some ground station. Other methods such as ultra-wideband (UWB) positioning do not rely on satellite connection but instead are purely based on ground stations, providing centimeter-level accuracy as well. Our position estimation algorithms must be able to read the sensor inputs and provide a position estimate that is accurate to within 0.1 meters of the actual estimate in order to enable our control algorithms to maintain a hover within a meter, as shown in our dynamics simulations.

D. Optimal Control

To maintain vehicle stability, we must find the optimal control inputs for the TVC and RCS system. Our RCS can be controlled via a lightweight bang-bang controller to maintain roll stability [23]. However, we need much more optimal control for the TVC to maintain a vertical attitude. We initially considered using proportional-integral-derivative (PID) and linear quadratic regulator (LQR) control. However, PID control is not well suited for the nonlinear dynamics that our vehicle will face [24]. LQR control was not able to properly account for effects such as the "tail-wags-dog" effect [25, 26]. We decided to use model predictive control (MPC) due to its superior capabilities for modeling such nonlinear effects and its ability to take into account future actions [27]. MPC works by simulating some time into the future and optimizing control over the entire sequence at the disadvantage of increased computing cost.

E. Thrust Vector Control

The majority of our control comes from our thrust vector control (TVC). The vehicle is capable of turning the engine to change the direction the thrust points, providing pitch and yaw control. However, to maintain a stable upright hover, we must be able to change the direction and magnitude of the thrust rapidly. Through empirical testing in our simulations, we determined that the TVC module must be able to actuate at a speed of at least 60 degrees per second and be able to reach an angle of at least 15 degrees from the vertical. This gives us the control authority to keep the vehicle stable throughout the entire flight profile. In addition to controlling the direction the engine gimbals, we must also control the thrust itself. Our main throttle valve (MTV) controls the oxidizer flow to the engine, modulating the thrust. This control is achieved through a PID controller augmented with a lookup table of valve angle to thrust values. The lookup table provides an estimate of the valve angle necessary and the PID controller provides fine adjustment on the valve angle to achieve more precise control. This arrangement allows for accurate and lightweight control on the MTV. We must have authority over our thrust to land without exceeding 0.5 meters per second. Otherwise, we risk structural damage. Therefore, our throttling algorithm must be able to achieve within 5% of the target thrust [28].

F. Reaction Control System

The vehicle's reaction control system (RCS) has authority over the roll axis, handling rotations the TVC is unable to correct. The requirements for the RCS are less stringent than the requirements for the thrust vector control system, since roll stability is less crucial than pitch or yaw stability. Instead of maintaining a precise angle, we can simply keep our roll angle within a set range. We have found through our dynamics simulations that maintaining the roll angle within 5 degrees of our starting angle keeps our angular velocity and vehicle attitude within constraints for both stable hovering and safe landing without damaging the landing gear.

G. Vehicle Navigation

While our MPC is able to provide optimal control within is look-ahead period, it fails to see the path as a whole. For that, we require a navigation algorithm to provide trajectories for the MPC to target and follow. There are several methods of solving the soft landing problem, which is a nonconvex problem, but the best solution for our case is lossless convexification (LCvx) due to its global optimality and guaranteed convergence. LCvx works by relaxing the constraints of the problem such that it becomes convex but the optimal solution remains the same as the original nonconvex problem's optimal solution [29]. This ensures that we do not discount any potential solutions. Additionally, since the problem is now convex, we can use efficient numerical solvers such as Clarabel to solve the problem, guaranteeing convergence within a given number of iterations. Nonlinear solving methods generally cannot guarantee convergence or optimality. LCvx neglects angular dynamics under the assumption that angular dynamics evolve much more quickly than translational ones, which is acceptable for a navigation algorithm since we have MPC to provide finer control. Because we make these assumptions, we must recalculate the trajectory in real time at a rate of at least 0.2 Hz to keep the error from the thrust constraint linear approximation under 0.5% [30].

H. Higher Level Control

To tie all of these algorithms together, we need an overarching control loop. To take advantage of all 6 CPU cores of the Jetson Orin Nano, our flight computer, we are multithreading our algorithms. This prevents algorithms with slower update rates like MPC or LCvx from holding up our faster updating sensor fusion algorithms. The control loop must enable all of our algorithms to reach their specified speeds while sharing variables between threads to keep a unified state estimate. A second responsibility of the control loop is maintaining communications with the ground station. The vehicle must send telemetry back to the ground station to allow us to monitor its condition and we must be able to send an emergency stop signal from the ground station back to the rocket. The rocket must also be able to self-terminate whenever flight conditions are deemed unsafe, however, these exact conditions will not be covered in this paper.

V. System Architecture

Figure 2. presents the integrated system architecture of the 1000N lander. The architecture is organized into 5 primary functional groupings: input modules (sensing), the main control loop, output actuation modules, power distribution, and ground communication. In this architecture, sensor measurements from the VN-300 GNSS/INS, pressure transducer, and backup IMU are first conditioned through the Data Interface Board before they are relayed to the Jetson Nano. Within the main control loop, these measurements are then fused to create an estimate of vehicle

states (position, velocity, attitude, and angular velocity). The estimated state is then provided to the navigation module which generates a reference trajectory using lossless convexification. At the end, the MPC controller then uses both the estimated state and the reference trajectory to compute updated optimal control inputs while respecting system constraints imposed by mainly the TVC and MTV. Finally, these control inputs are then sent to the output layer where TVC receives the required position for pitch and yaw, the MTV for valve angle as a means to control thrust magnitude, and RCS for pulse durations. The resulting thrust and roll corrections then alters the vehicle state which closes the feedback loop to the sensing layer to complete the system cycle.

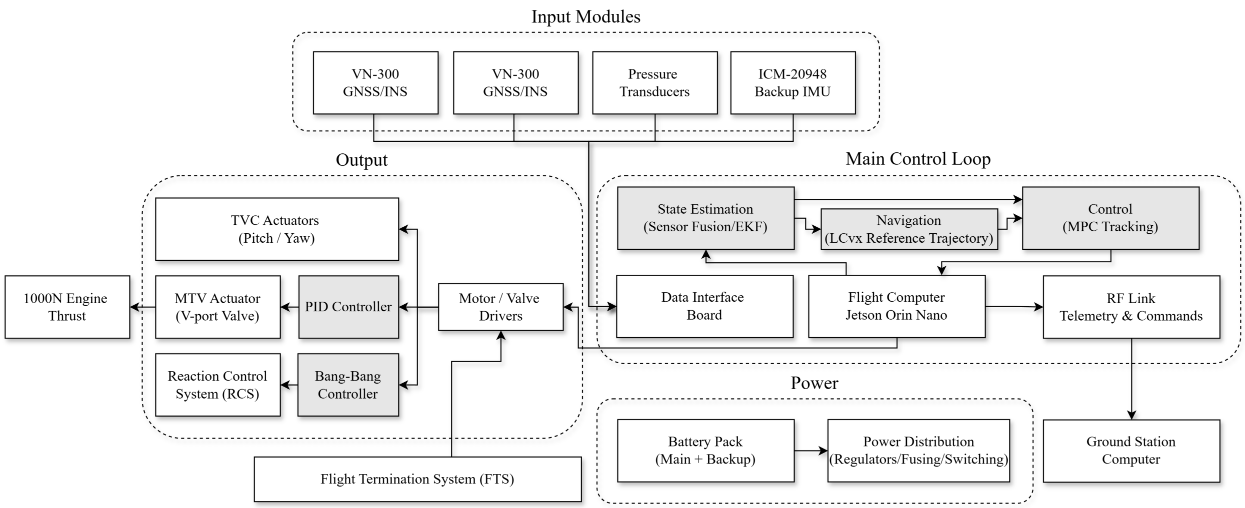

Fig. 2 System Architecture of Lander

VI. Conclusions

To the authors' knowledge, present hybrid VTVL demonstrations have been limited to constrained to tethered hover tests and single-degree-of-freedom altitude-control experiments. Publicly documented demonstrations of an untethered vertical hop and powered descent using a throttle-regulated hybrid propulsion system are absent in the open literature. While hybrid engines have been extensively investigated for ascent purposes, their use in closed-loop, free-flight powered descent remains largely unexplored. The architecture presented here was therefore developed to evaluate the feasibility of hybrid propulsion in untethered VTVL flight with full guidance, navigation, and control authority.

Acknowledgments

The authors would like to acknowledge the Georgia Institute of Technology for providing the institutional support, facilities, and academic environment that make student-led aerospace research possible. This work represents the collective effort of Propulsive Landers at Georgia Tech (GTPL). The authors sincerely thank the members of GTPL for their contributions, long test days, and continued commitment to advancing reusable rocketry at the student scale.

References

[1] American Institute of Aeronautics and Astronautics, "Spaceport America Cup," , Jul. 2025. URL `https://aiaa.org/events/spaceport-america-cup/`.

[2] Clark College, "Spaceport America Cup," , 2024. URL `https://www.clark.edu/news-and-media/24-7/2024/06/Spaceport-America-Cup.php`.

[3] Taiwan Space Agency, "1st Rocket Taiwan Cup Competition Concludes, Igniting Youth's Space Dreams," , ???? URL `https://www.tasa.org.tw/en-US/announcements/detail/50752326-9aea-4e56-9de1-235fd56127f4`.

[4] SpaceX, "Starship," , 2025. URL `https://www.spacex.com/vehicles/starship`.

[5] Blue Origin, "New Glenn Launches NASA's ESCAPADE, Lands Fully Reusable Booster," , 2025. URL `https://www.blueorigin.com/news/new-glenn-launches-nasa-escapade-lands-fully-reusable-booster`.

[6] European Space Agency, "Themis," , 2022. URL https://www.esa.int/Enabling_Support/Space_Transportation/Themis.
[7] LandSpace, "Chinese Private Space Company Completes Vertical Takeoff and Landing Test for Reusable Rocket," , 2024. URL https://www.landspace.com/en/news-detail.html.
[8] Wei, S.-S., Li, M.-C., Lai, A., Chou, T.-H., and Wu, J.-S., "A Review of Recent Developments in Hybrid Rocket Propulsion and Its Applications," *Aerospace*, Vol. 11, 2024, p. 739. https://doi.org/10.3390/aerospace11090739, URL https://www.mdpi.com/2226-4310/11/9/739.
[9] Armand, R., *Nitrous Oxide/Paraffin Hybrid Rocket Engines*, 2010.
[10] Palacz, T., "Nitrous Oxide Application for Low-Thrust and Low-Cost Liquid Rocket Engine," *9th European Conference for AeroSpace Sciences (EUCASS)*, 2017. https://doi.org/10.13009/EUCASS2017-474, URL https://www.eucass.eu/doi/EUCASS2017-474.pdf.
[11] Whitmore, S. A., , Z., and Eilers, S. D., "Closed-Loop Precision Throttling of a Hybrid Rocket Motor," Vol. 30, 2014, pp. 325–336. https://doi.org/10.2514/1.b34924.
[12] Karabeyoglu, A., Zilliac, G., Cantwell, B. J., DeZilwa, S., and Castellucci, P., "Scale-Up Tests of High Regression Rate Paraffin-Based Hybrid Rocket Fuels," *Journal of Propulsion and Power*, Vol. 20, 2004, pp. 1037–1045. https://doi.org/10.2514/1.3340.
[13] Karabeyoglu, M. A., Altman, D., and Cantwell, B. J., "Combustion of Liquefying Hybrid Propellants: Part 1, General Theory," *Journal of Propulsion and Power*, Vol. 18, 2002, pp. 610–620. https://doi.org/10.2514/2.5975.
[14] Bisin, R., Paravan, C., Verga, A., and Galfetti, L., "Towards High-Performing Paraffin-Based Fuels Exploiting the Armored Grain Concept," *10th European Conference for AeroSpace Sciences (EUCASS)*, 2022. https://doi.org/10.13009/EUCASS2022-4860, URL https://www.eucass.eu/doi/EUCASS2022-4860.pdf.
[15] Atkinson, C., Lai, K., and Soria, J., "ABS Infill Structures for Enhancing the Performance of Paraffin Fuel Grains in Hybrid Rocket Engines," , 2022. https://doi.org/10.26180/19761427.
[16] Eilers, S. D., and Whitmore, S. A., "Correlation of Hybrid Rocket Propellant Regression Measurements with Enthalpy-Balance Model Predictions," *Journal of Spacecraft and Rockets*, 2024. https://doi.org/10.2514/1.33804.
[17] Gerbal, N., Durand, G., Avril, M., Lefranc, L., Vautier, C., Chergui, B., Diop, M., Feroldi, G., Deroo, M., Diakuma, J., Le Moguédec, P., Tahan, Q., Ansart, A., Diallo, T., Sire, G., and Poirey, G., "Formulation of a Mechanically Improved Paraffin Fuel," *Proceedings of the 5th European Conference for Aeronautics and Space Sciences (EUCASS)*, EUCASS, Munich, Germany, 2013.
[18] Bouziane, M., Bertoldi, A., Milova, P., Hendrick, P., and Lefebvre, M., "Performance comparison of oxidizer injectors in a 1-kN paraffin-fueled hybrid rocket motor," *Aerospace Science and Technology*, Vol. 89, 2019, pp. 392–406. https://doi.org/10.1016/j.ast.2019.04.009.
[19] Mechentel, F. S., and Cantwell, B. J., "Experimental Findings on Pre- and Post-combustion Chamber Effects in a Laboratory-scale Motor," *AIAA Propulsion and Energy 2019 Forum*, 2019. https://doi.org/https://doi.org/10.2514/6.2019-4336.
[20] Li, M.-C., Chang, C.-S., Wei, S.-S., and Wu, J.-S., "Experimental Investigation of Throttleable H2O2 and Polypropylene Hybrid Rocket Motor," *Journal of Propulsion and Power*, Vol. 39, 2023, pp. 63–70. https://doi.org/10.2514/1.b38720.
[21] Marquardt, T. A., and Majdalani, J., "A Primer on Classical Regression Rate Modeling in Hybrid Rockets," *AIAA Propulsion and Energy 2020 Forum*, 2020.
[22] Peterson, Z. W., Eilers, S. D., and Whitmore, S. A., "Closed-Loop Thrust and Pressure Profile Throttling of a Nitrous-Oxide HTPB Hybrid Rocket Motor," *48th AIAA/ASME/SAE/ASEE Joint Propulsion Conference and Exhibit*, American Institute of Aeronautics and Astronautics, Atlanta, Georgia, 2012. https://doi.org/10.2514/6.2012-4200.
[23] Song, G., Buck, N. V., and Agrawal, B. N., "Spacecraft Vibration Reduction Using Pulse-Width Pulse-Frequency Modulated Input Shaper," *Journal of Guidance, Control, and Dynamics*, Vol. 22, No. 3, 1999, pp. 433–440. https://doi.org/10.2514/2.4415.
[24] Bouabdallah, S., Noth, A., and Siegwart, R., "PID vs LQ control techniques applied to an indoor micro quadrotor," *2004 IEEE/RSJ International Conference on Intelligent Robots and Systems (IROS)*, Vol. 3, 2004, pp. 2451–2456. https://doi.org/10.1109/IROS.2004.1389776.
[25] Waslander, S. L., Hoffmann, G. M., Jang, J. S., and Tomlin, C. J., "Multi-agent X4-flyer testbed control design: integral sliding mode vs. LQR," *AIAA Infotech@Aerospace*, 2005, p. 7043. https://doi.org/10.2514/6.2005-7043.
[26] Greensite, A. L., "Analysis and Design of Space Vehicle Flight Control Systems: Vol. VII - Attitude Control During Launch," Tech. Rep. NASA CR-826, National Aeronautics and Space Administration, 1967.
[27] Eren, U., Prach, A., Koçer, B. B., Kuroe, Y., Bogdan, S., Dickeson, J. V., et al., "Model Predictive Control in Aerospace Systems: Current State and Opportunities," *Journal of Guidance, Control, and Dynamics*, Vol. 40, No. 7, 2017, pp. 1541–1566. https://doi.org/10.2514/1.G002507.
[28] Kuran, B., "Fault Tolerant Convex Guidance for Lunar Powered Descent," Master's thesis, Middle East Technical University, 2024.
[29] Açıkmeşe, C. J. M. I., B., and Ploen, S. R., "Lossless Convexification of Nonconvex Control Bound and Pointing Constraints of the Soft Landing Optimal Control Problem," *IEEE Transactions on Control Systems Technology*, Vol. 21, 2013. https://doi.org/10.1109/TCST.2012.2237346.
[30] Açıkmeşe, B., and Ploen, S. R., "Convex Programming Approach to Powered Descent Guidance for Mars Landing," *Journal of Guidance, Control, and Dynamics*, Vol. 30, 2007. https://doi.org/10.2514/1.27553.